Proceedings of 8th International Conference on Mechanical Engineering and Renewable Energy 2025
10-12 December, 2025, Chattogram, BANGLADESH

SciEn Conference Series: Engineering Vol. 4, 2026, pp 330-335 https://doi.org/10.38032/scse.2026.4.151

Aerodynamic Assessment of Leading-edge Tubercles on Variable-Camber NACA X410 Airfoils: A CFD Study

Md. Jubayer Hasan Jim, Zannatul Mim and Nusrat Nawar Ahsan*

Department of Mechanical Engineering, Rajshahi University of Engineering and Technology, Rajshahi-6204, Bangladesh

ABSTRACT

The humpback whale represents a key example of bio-inspired engineering, with leading-edge tubercles on its flippers enhancing hydrodynamic efficiency and maneuverability. Inspired by this natural adaptation, the present study examines the aerodynamic implications of incorporating leading-edge tubercles into airfoil designs. NACA X410 airfoils (NACA 1410, NACA 2410, and NACA 4410) were selected for modification with leading-edge tubercles and then investigated through numerical simulations. The airfoils had a chord and span length of 1 m, with tubercles having a wavelength of 200 mm and an amplitude of 25 mm. A three-dimensional steady-state analysis was performed using the viscous SST k-ω turbulence model in ANSYS Fluent. The tubercled NACA 4410 exhibited the highest lift-to-drag ratio among all tubercled profiles. Velocity and pressure contours were analyzed to illustrate the distribution of positive and negative pressures, as well as flow velocity around the airfoils. Further research can be conducted on this topic by exploring varying camber sizes.

Keywords: Airfoil, Tubercles, Aerodynamics, Lift-to-drag ratio, Numerical simulation.

1. Introduction

Global energy demand is rising rapidly, increasing the need for renewable energy sources like wind energy[1]. Wind energy is one of the fastest-growing renewable sources due to its sustainability and low cost. Wind energy is primarily harnessed through wind turbines, whose efficiency is strongly influenced by blade geometry. Numerous studies have demonstrated that airfoil performance can be enhanced through biomimetic or nature-inspired designs. The exceptional maneuverability of humpback whales is attributed to tubercles; large, rounded protrusions along the leading edge of their flippers, which have inspired the development of bio-inspired wing designs. The investigations of Watts and Fish[2] demonstrated that tubercles enhance beneficial force generation while simultaneously reducing parasitic forces[3]. The results demonstrate that the lift coefficient of the modified airfoils is enhanced to a certain extent after these airfoils stall.[3] The work of Zao Ni et al. demonstrated that for NACA 634–021 airfoil with leading-edge tubercles and an internal slot exhibit significant lift and drag improvement at angles of attack above 10°[4]. The work of B. K. Sreejith demonstrated that tubercled E216 airfoils generate higher lift than the plain airfoil in the pre-stall region but lower lift at the stall angle, with a maximum Cl improvement of 4.51% observed for the airfoil with 8 mm amplitude and 64 mm wavelength at 6° angle of attack[5].

Fig.1(a) illustrates the publication trends from 2016 to 2025, based on the keywords 'airfoil performance enhancement' and 'airfoil tubercles' in abstracts or titles. As observed, relatively few studies have focused on performance enhancement through tubercles compared to general airfoil modifications.

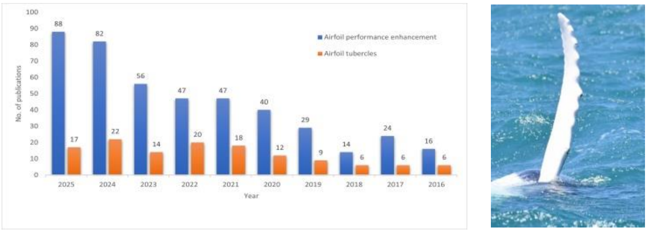

(a) (b)

Fig. 1 (a)Recent trend in the publications on airfoil modifications (airfoil performance enhancement and airfoil tubercles) (b)Image of a humpback whale fin and it's tubercles.

1.1 Recent advances on tubercled airfoil.

Despite these advances, the interaction between tubercle geometry and airfoil camber is not fully understood. While many studies report stall delay, some, particularly those using steady-state Reynolds-Averaged Navier-Stokes (RANS) simulations, have observed contradictory trends, suggesting that the flow physics may be more complex and dependent on specific geometric and flow parameters[9]. This study aims to address this gap by systematically investigating the effect of leading-edge tubercles on three airfoils from the NACA X410 series with varying camber (NACA 1410, 2410, 4410). The novelty of this work lies in its focused examination of how camber variation within a symmetric-thickness airfoil family influences the efficacy of a fixed tubercle geometry.

*Corresponding Author Email Address: jubayerhasan.me21@gmail.com Published By: SciEn Publishing Group

Table 1 Recent Research on Leading edge tubercles.

Passive Control Method	Reported Effect	Ref.
Leading-edge tubercles	The tubercled airfoil exhibited a stall angle of 18 degrees, with the maximum lift coefficient observed at a freestream velocity of 20 m/s across the tested range of -30m/s to 30 m/s.	[6]
Leading-edge tubercles	For NACA 24XX airfoils, the tubercled NACA 2410 exhibited a 24.09% higher Cl/Cd compared to the non-tubercled configuration, indicating a significant aerodynamic improvement.	[7]
Leading-edge tubercles	The reference airfoil stalls sharply at 18°, while Mod-1 delays stall with higher lift and lower drag, and Mod-2 trades stall performance for lift due to counter-rotating vortex pairs. Both modified airfoils outperform the reference in the post-stall region.	[3]
Tubercles on leading edge	The modified airfoil with leading-edge tubercles, were tested in a Göttingen-type circular wind tunnel using tuft visualization, showed smoother stall and improved post-stall performance as the tubercles act like a series of delta wings along the leading edge though pre-stall performance decreased.	[8]

2. Methodology

2.1 Airfoil Geometry and Creation

Three NACA X410 airfoils (NACA 1410, NACA 2410, and NACA 4410) were selected for this study, with varying camber sizes. Airfoil coordinates were obtained from the Airfoil Tools website, and the airfoils were modeled using SolidWorks. For non-tubercled airfoils, the sketches were extruded along the z-axis, with both chord and span lengths set to 1 m. Tubercles were added to the leading edge of the airfoils using the loft feature, with a wavelength of 200 mm and an amplitude of 25 mm, as these parameters yielded the highest aerodynamic performance in the study by Cameo and Harnez[7]. All three airfoils were modified using the same wavelength and amplitude parameters, as illustrated in Fig. 2.

2.2 Experimental Setup and Procedure

All analysis were performed using the ANSYS suite of computational fluid dynamics software, specifically ANSYS DesignModeler for geometry and domain creation, and ANSYS Fluent for meshing and flow simulations. ANSYS Fluent analyzes the fluid domain; therefore, a wind tunnel test section was created around the airfoil, with a rectangular domain extending 10 chord lengths upstream of the leading edge and 20 chord lengths downstream of the trailing edge (Fig.3(a)).

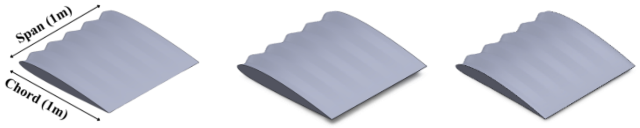

(a)NACA 1410 (b)NACA 2410 (c)NACA 4410

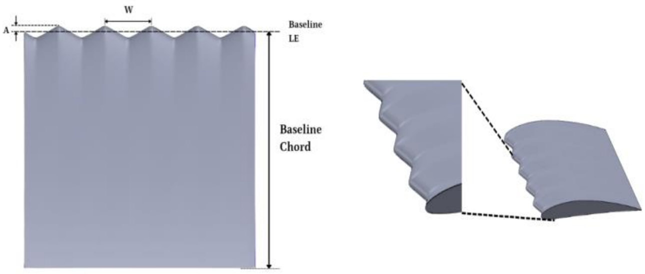

(d)Parameters of tubercled blade. (e)Leading age Tubercles.

Fig. 2 Single-blade geometries of tubercles airfoils.

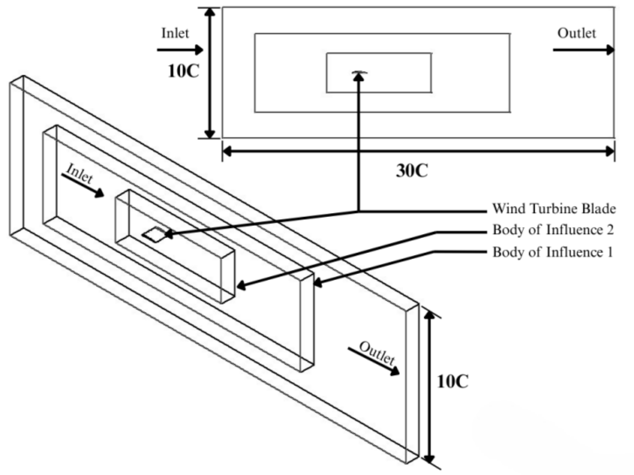

(a)

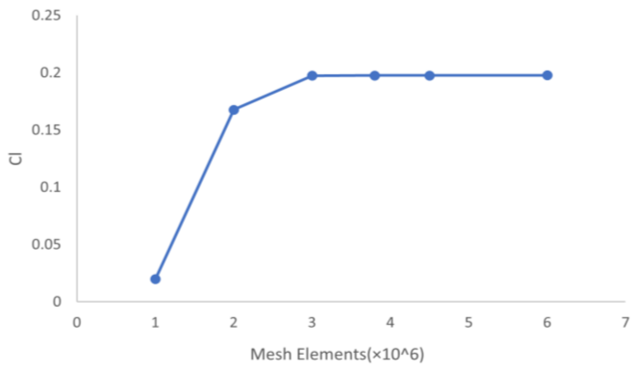

(b)

Fig. 3 (a)Dimensions of the computational domain, (b)Mesh Dependency Analysis.

The airfoil geometry was subtracted from the computational domain. Three computational domains were used to determine appropriate element sizes for meshing. The mesh was composed primarily of tetrahedral elements with an inflation layer comprising 10 prismatic layers around the airfoil surface to resolve the boundary layer accurately. The first layer thickness was set to achieve a non-dimensional wall distance $y^+ \approx 1$ suitable for the SST k-ω model which resolves the flow down to the viscous sublayer. Edge, face, and body sizes were selected based on mesh dependency analysis (Fig.3(b)), and suitable mesh quality metrics were ensured (maximum skewness 0.81, minimum orthogonal quality 0.23). The smallest mesh element measured 0.001 m, and approximately 3.8 million elements were used for the simulations (Fig.4).

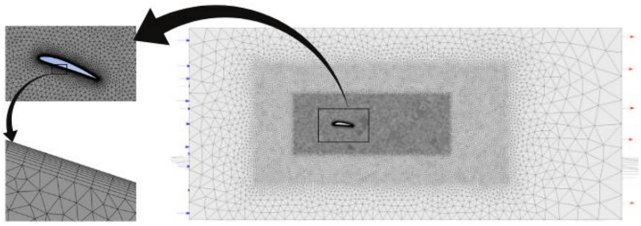

Fig.4 Final mesh quality and mesh with inflation layers.

A steady-state analysis of the selected airfoils was conducted using the viscous SST k-ω model. Air was defined as the working fluid, with a density of 1.205 kg/m³ and dynamic viscosity of 1.82×10^{-5} kg/ms, as summarized in Table 1, which also provides reference values for calculating lift and drag coefficients. The freestream velocity was set to 7 m/s. The inlet turbulence intensity and viscosity ratio were maintained at their default values for the simulation. Symmetry boundary conditions were imposed on the upper and lower surfaces of the computational domain to emulate an infinite-span configuration and eliminate spanwise flow variations. This procedure was repeated for both modified and unmodified NACA 1410, 2410, and 4410 airfoils at various angles of attack. A maximum of 600 iterations was allowed, although convergence was typically achieved within 150 iterations.

Table 2 Overview of the key parameters of numerical investigation.

Parameter	Value/Type	Parameter	Value/Type
Analysis Type	Steady	Reynolds Number	4.6×10^5
Viscous Model	SST k-ω	Fluid Viscosity	1.82×10^{-5} kg/ms
Fluid Velocity	7 m/s	Fluid Density	1.205 kg/m^3
Reference Values	Compute from inlet Area- 1m^2 Length- 1m	Method	2nd Order upwind
Residual Conver -gence	10^{-6}	Pressure -Velocity Coupling	(Coupled)
Boundary Condition	Inlet-velocity inlet Outlet- Pressure outlet Wall- No slip	Pressure	PRESTO!

2.3 Validation

To validate the numerical setup, the baseline NACA 2410 airfoil was simulated and its results were compared against well-established data from XFOIL [10] and the experimental data of Cameo Hernanz et al.[7] where an inlet velocity of 65 m/s and a dynamic viscosity of 1.789×10^{-5} Pa·s were employed, as illustrated in Fig. 5.

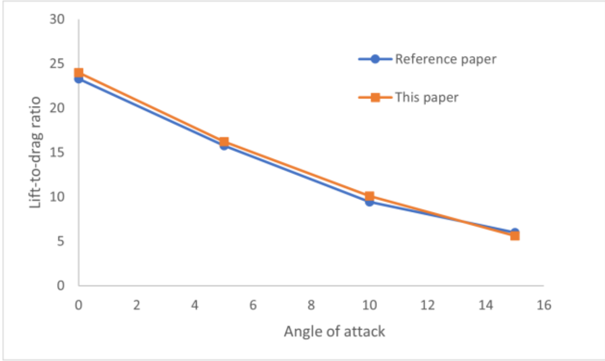

Fig. 5 Comparison of simulation parameters with reference validation study.

3. Results and Discussion

The numerical analysis of the selected airfoils is presented in the (Fig.6 and Fig.7). This study numerically investigates three airfoils: NACA 1410, NACA 2410, and NACA 4410 with varying camber sizes, comparing their performance with and without leading-edge tubercles. For non-tubercled airfoils, the stall angle was observed at 15 degrees, whereas tubercled airfoils exhibited stall at an angle of attack of 10 degrees. However, the maximum lift-to-drag ratio was obtained at 5 degrees for both tubercled and non-tubercled airfoils. The highest lift-to-drag ratio of 36.2299 was achieved by the non-tubercled NACA 2410, whereas reductions of 28.73% and 17.6% were observed for the non-tubercled NACA 1410 and NACA 4410, respectively. Thus, no continuous trend was observed with increasing camber size. Similar to the other airfoils, the lift coefficient for both tubercled and non-tubercled airfoils increases up to the stall angle, after which it decreases, while the drag coefficient rises steadily with the angle of attack.

A notable observation is that the lift coefficient at the stall angle for tubercled airfoils gradually increases with increasing camber size. Among the tubercled airfoils, NACA 4410 exhibited the highest lift coefficient (1.0908) and lift-to-drag ratio (32.89). The tubercled NACA 4410 demonstrates a 9.24% performance increase compared to the non-tubercled NACA 4410, whereas the tubercled NACA 1410 shows only a 2.74% improvement. In contrast, the tubercled NACA 2410 shows a significant performance reduction compared to the non-tubercled configuration. In this study, the authors of NACA X410 airfoils, both tubercled and non-tubercled, revealing an optimum operating point at 5 degree angle of attack for the tubercled NACA 4410 compared to the non-tubercled configurations.

Fig.8 presents the pressure contour plots on a cross-sectional plane at the mid-span of the airfoil. It indicates that NACA 4410 (Fig.8(c)), exhibits a substantial negative pressure distribution on the upper surface of the airfoil compared to the other two airfoils. Consequently, NACA 4410 generates a greater pressure difference between the upper and lower surfaces, producing an increased upward force and higher lift. In contrast, NACA2410 (Fig.8(b)), exhibits minimal pressure variation between the suction and pressure surfaces, resulting in the lowest lift among the configurations. Therefore, this configuration generates the lowest lift among all the blade configurations. For NACA 1410 (Fig.8(a)) the pressure distribution is higher than the NACA2410 (Fig.8(b)), but slightly lower than the NACA 4410 (Fig.8(c)).

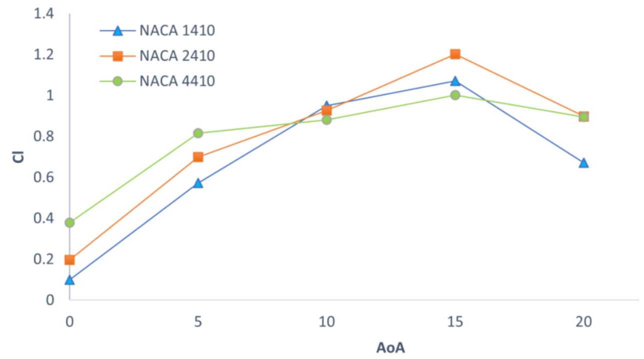

(a)

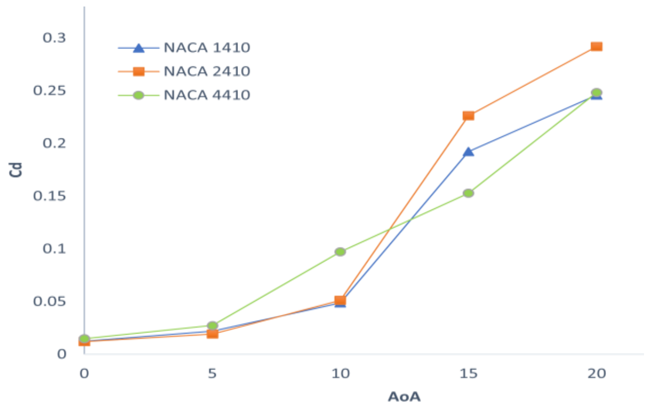

(b)

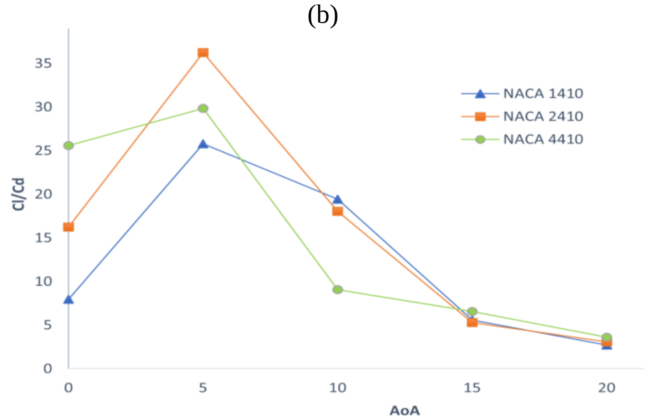

(c)

Fig.6 Variation of (a) Lift coefficient (CL), (b) Drag coefficient (CD), (c) Lift to-drag ratio (L/D) with the angle of attacks for the non-tubercled airfoils.

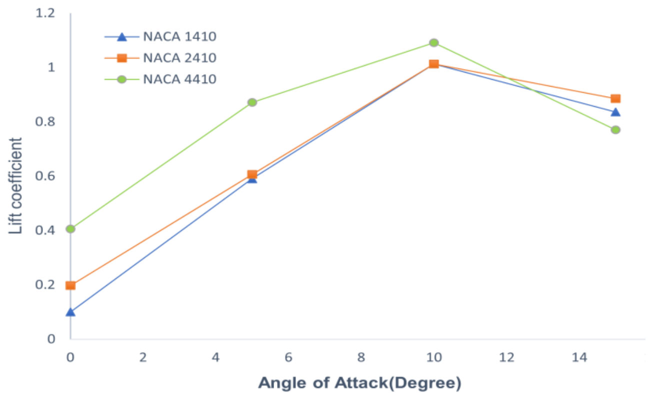

(a)

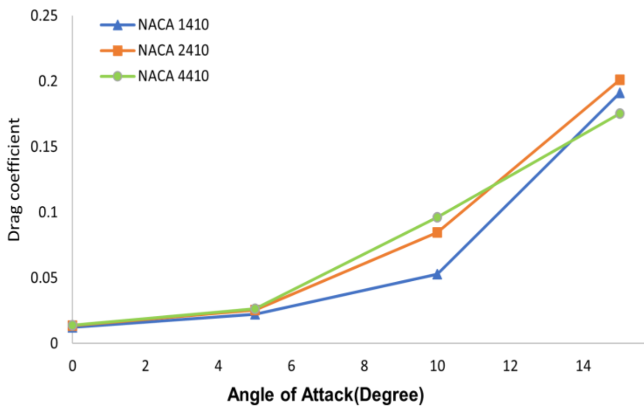

(b)

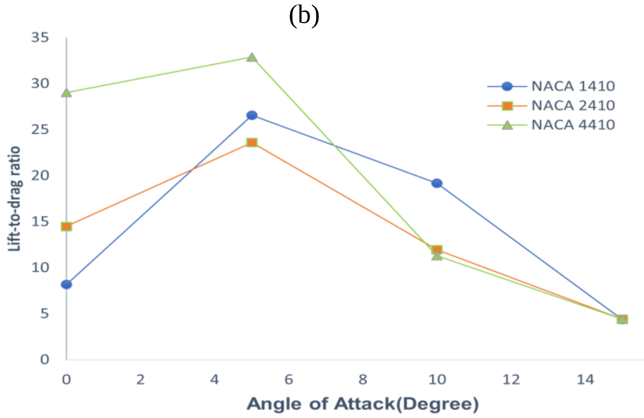

(c)

Fig.7 Variation of (a) Lift coefficient (CL), (b) Drag coefficient (CD), (c) Lift to-drag ratio (L/D) with the angle of attacks for the tubercled airfoils.

The velocity contour plot for three different airfoils are presented in Figure 9, using the midplane of the blade as a reference. In Fig. 9(c), NACA 4410 exhibits the strongest velocity increase above the airfoil (largest red zone), producing the greatest suction effect and highest lift, although a more pronounced wake indicates increased drag.

In contrast, NACA 2410 (Fig. 9(b)) shows minimal pressure variation between the suction and pressure surfaces, leading to the lowest lift among the configurations. Compared to the other two airfoils, NACA 1410 (Fig. 9(a)) exhibits moderate acceleration on the upper surface and a downstream wake, resulting in intermediate drag.

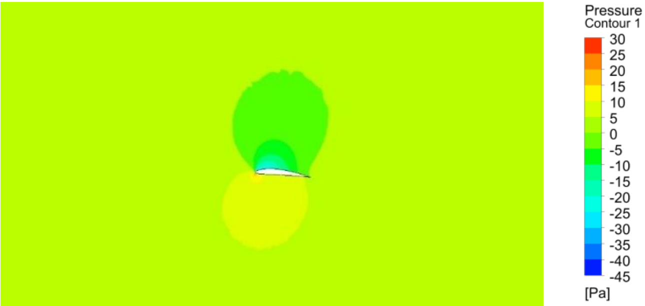

(a)NACA1410

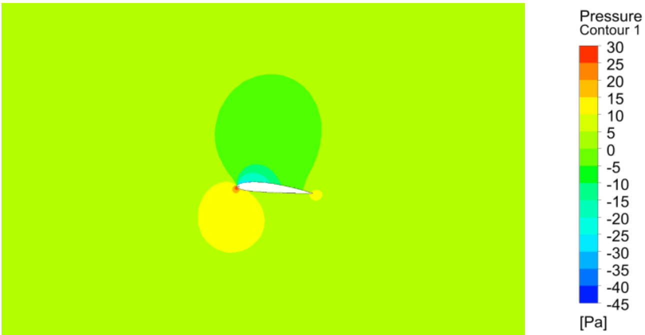

(b)NACA2410

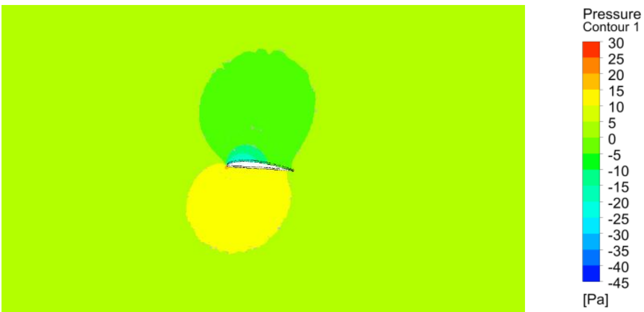

(c)NACA4410

Fig. 8 Pressure Contour of NACA X410 airfoils at 5-degree AoA.

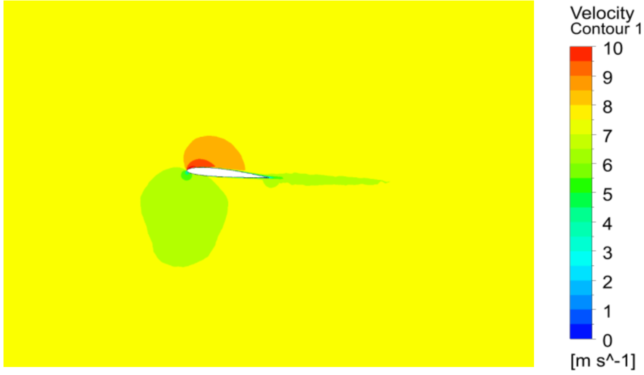

(a)NACA1410

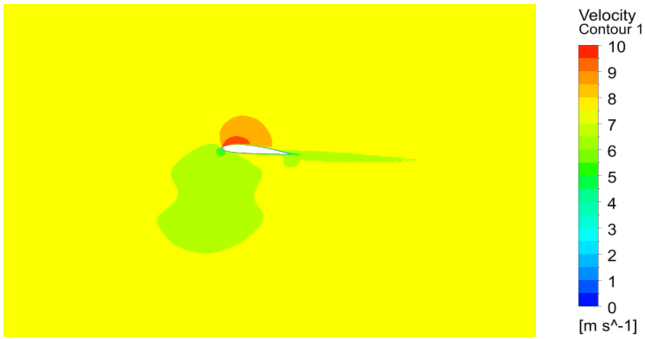

(b)NACA2410

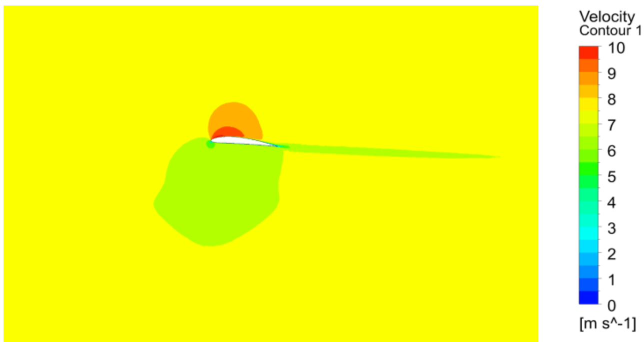

(c)NACA4410

Fig. 9 Velocity Contour of NACA X410 airfoils at 5-degree AoA.

4. Conclusion

This study investigates three asymmetric airfoils with varying camber sizes from the four-digit NACA X410 series and provides significant insights into lift generation and lift-to-drag ratio. NACA 1410, NACA 2410, and NACA 4410 airfoils, both with and without tubercles, were numerically investigated to evaluate and compare their aerodynamic characteristics across different angles of attack. The study revealed that the tubercled NACA 4410 airfoil achieved the highest lift coefficient of 1.0908 at 10° angle of attack, while the maximum lift-to-drag ratio of 32.89 was observed at 5° angle of attack.

Similar to the non-tubercled airfoils, the tubercled configurations did not exhibit a continuous variation in lift-to-drag ratio with increasing camber size. The NACA 4410 demonstrated a 39.3% performance increase compared to NACA 2410 and a 23.89% increase relative to NACA 1410. Ultimately, the tubercled NACA 4410 outperformed its non-tubercled form by 9.24%, while NACA 1410 showed only a 2.74% improvement. In contrast, NACA 2410 exhibited a performance reduction within the parameter range investigated in this study. In the study by Cameo Hernanz et al.[7], the tubercled NACA 2410 airfoil exhibited a 24.09% increase in lift-to-drag ratio.

Conversely, the present work observed a reduction in aerodynamic performance for the same airfoil, likely due to variations in the numerical setup, boundary conditions, and flow parameters between the two studies. Moreover, pressure and velocity contour plots were presented to provide deeper insight into the mechanisms of lift generation for both modified and unmodified NACA X410 airfoils. Future research on tubercled airfoils may focus on optimizing tubercle wavelength and amplitude across varying camber sizes to achieve improved aerodynamic performance. Fig.10 illustrates the comparison between lift-to-drag ratio for tubercled and non-tubercled airfoils.

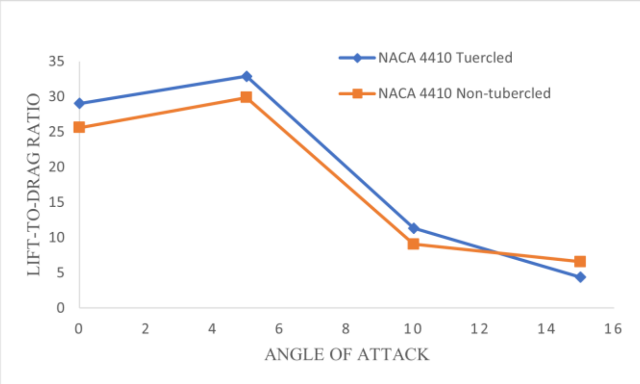

Fig. 10 Lift-to-drag ratio for tubercled and non_tubercled airfoils with angle of attack.

5. References

[1] S. Roga, S. Bardhan, Y. Kumar, and S. K. Dubey, "Recent technology and challenges of wind energy generation: A review," *Sustain. Energy Technol. Assess.*, vol. 52, p. 102239, Aug. 2022, doi: 10.1016/j.seta.2022.102239.

[2] "[PDF] THE INFLUENCE OF PASSIVE , LEADING EDGE TUBERCLES ON WING PERFORMANCE | Semantic Scholar." Accessed: Jan. 27, 2026. [Online]. Available: https://www.semanticscholar.org/paper/THE-INFLUENCE-OF-PASSIVE-,-LEADING-EDGE-TUBERCLES-Watts/1e5a294c53043a40e0f0ff3bebfcfe795c90a202

[3] M. Fan, X. Dong, Z. Li, Z. Sun, and L. Feng, "Numerical and experimental study on flow separation control of airfoils with various leading-edge tubercles," *Ocean Eng.*, vol. 252, p. 111046, May 2022, doi: 10.1016/j.oceaneng.2022.111046.

[4] Z. Ni, M. Dhanak, and T. Su, "Performance Characteristics of Airfoils with Leading-Edge Tubercles and an Internal Slot," *AIAA J.*, vol. 57, no. 6, pp. 2394–2407, Jun. 2019, doi: 10.2514/1.J058145.

[5] B. K. Sreejith and A. Sathyabhama, "Experimental and numerical study of laminar separation bubble formation on low Reynolds number airfoil with leading-edge tubercles," *J. Braz. Soc. Mech. Sci. Eng.*, vol. 42, no. 4, p. 171, Apr. 2020, doi: 10.1007/s40430-020-2229-2.

[6] G. Balaji, S. Gupta, G. K. Manikpuri, S. Sureshkumar, S. Sathish, and V. Madhanraj, "Numerical investigation of aerodynamic performance of leading edge tubercle airfoil at low Reynolds number," *Mater. Today Proc.*, vol. 68, pp. 1455–1465, 2022, doi: 10.1016/j.matpr.2022.07.005.

[7] A. Cameo Hernanz and T. Janshon, "Investigating the Tubercle Effect on the NACA 24xx airfoil series: Investigation Using Ansys Fluent," in *2024 Regional Student Conferences*, Multiple Locations: American Institute of Aeronautics and Astronautics, Jan. 2024. doi: 10.2514/6.2024-80551.

[8] D. Wang *et al.*, "Impact of Leading-Edge Tubercles on Airfoil Aerodynamic Performance and Flow Patterns at Different Reynolds Numbers," *Energies*, vol. 17, no. 21, p. 5518, Nov. 2024, doi: 10.3390/en17215518.

[9] N. Rostamzadeh, R. M. Kelso, and B. Dally, "A numerical investigation into the effects of Reynolds number on the flow mechanism induced by a tubercled leading edge," *Theor. Comput. Fluid Dyn.*, vol. 31, no. 1, pp. 1–32, Feb. 2017, doi: 10.1007/s00162-016-0393-x.

[10] M. Drela, "XFOIL: An Analysis and Design System for Low Reynolds Number Airfoils," in *Low Reynolds Number Aerodynamics*, vol. 54, T. J. Mueller, Ed., in Lecture Notes in Engineering, vol. 54. , Berlin, Heidelberg: Springer Berlin Heidelberg, 1989, pp. 1–12. doi: 10.1007/978-3-642-84010-4_1.